

# Multistability and arithmetically period-adding bifurcations in piecewise smooth dynamical systems

Younghae Do<sup>1</sup> and Ying-Cheng Lai<sup>2</sup>

<sup>1</sup>*Department of Mathematics, Kyungpook National University, Daegu 702-701, South Korea*

<sup>2</sup>*Department of Electrical Engineering and Department of Physics, Arizona State University, Tempe, Arizona 85287, USA*

(Received 3 June 2008; accepted 27 August 2008; published online 15 October 2008)

Multistability has been a phenomenon of continuous interest in nonlinear dynamics. Most existing works so far have focused on smooth dynamical systems. Motivated by the fact that nonsmooth dynamical systems can arise commonly in realistic physical and engineering applications such as impact oscillators and switching electronic circuits, we investigate multistability in such systems. In particular, we consider a generic class of piecewise smooth dynamical systems expressed in normal form but representative of nonsmooth systems in realistic situations, and focus on the weakly dissipative regime and the Hamiltonian limit. We find that, as the Hamiltonian limit is approached, periodic attractors can be generated through a series of saddle-node bifurcations. A striking phenomenon is that the periods of the newly created attractors follow an arithmetic sequence. This has no counterpart in smooth dynamical systems. We provide physical analyses, numerical computations, and rigorous mathematical arguments to substantiate the finding. © 2008 American Institute of Physics. [DOI: 10.1063/1.2985853]

**Multistability, as characterized by the coexistence of multiple attractors, is common in nonlinear dynamical systems. In such a case, starting the system from a different initial condition can result in a completely different final or asymptotic state. The behavior thus has implications to fundamental issues such as repeatability in experimental science. Existing works on multistability in nonlinear dynamics focus mostly on smooth systems. A typical scenario for multistability to arise is when a Hamiltonian system becomes weakly dissipative so that a large number of Kol'mogorov–Arnol'd–Moser (KAM) islands become sinks, or stable periodic attractors. There has also been an interest in nonsmooth dynamical systems. For example, piecewise smooth systems have been known to arise commonly in physical and engineering contexts such as impact oscillators and switching circuits. Previous works have shown that nonsmooth dynamical systems can exhibit bifurcations that have no counterparts in smooth systems. The aim of this paper is to explore general phenomena associated with multistability in nonsmooth dynamical systems. We shall use a generic class of piecewise smooth maps that are representative of nonsmooth dynamical systems. By focusing on the weakly dissipative regime near the Hamiltonian limit, we find that multistability can arise as a result of various saddle-node bifurcations. A striking phenomenon is that, as a parameter characterizing the amount of the dissipation is decreased, the periods of the stable periodic attractors created at the sequence of saddle-node bifurcations follow an arithmetic order. We call such bifurcations “arithmetically period-adding bifurcations.” We provide physical analyses, numerical computations, and mathematical proofs to establish the occurrence of these bifurcations.**

**Our work reveals that multistability can be common in nonsmooth dynamical systems, and its characteristics can be quite different from those in smooth dynamical systems.**

## I. INTRODUCTION

Nonlinear dynamical systems exhibit rich long-term behaviors such as stationary, periodic, quasiperiodic, and chaotic attractors. Many systems in nature and technological applications share the trait that, for a given set of parameters, there can be more than one attractor or asymptotic state, each with its own basin of attraction. As a result, such a system, when starting from different initial conditions, can evolve into different attractors with completely different long-term behaviors. The situation can also arise that the number of coexisting attractors is large. This phenomenon is called multistability and it occurs in many fields of science and engineering.<sup>1–3</sup>

The dynamics of systems exhibiting multistability have attracted continuous interest.<sup>4–9</sup> One typical scenario by which many attractors, usually periodic ones, can arise in the phase space is through weak dissipation in a Hamiltonian system. In the absence of dissipation, the system is conservative and its phase space is typically occupied by a mixture of infinite hierarchies of Kol'mogorov–Arnol'd–Moser (KAM) islands and chaotic seas. When a small amount of dissipation is introduced, the KAM islands are turned into sinks, generating an infinite number of periodic attractors in the phase space, and the original chaotic seas become effectively basin boundaries. As a result, the basins of attraction of the attractors are interwoven in an extremely complicated

manner,<sup>4-8</sup> and the basin boundaries permeate most of the phase space, except for small open neighborhoods about the periodic attractors. The fractal dimensions of the basin boundaries are close to the dimension of the phase space.

The purpose of this paper is to explore multistability in nonsmooth dynamical systems that arise commonly in physical and engineering devices such as impact oscillators<sup>2</sup> and electronic circuits.<sup>3</sup> In particular, we shall consider a generic class of piecewise smooth systems.<sup>10-16</sup> For such a system, the phase space can be divided into two regions where the dynamics in each region are different from each other but are nonetheless smooth, and a border that separates the two regions. This setting is representative of physical systems such as switch electronic circuits,<sup>3</sup> and previous mathematical analyses have revealed interesting phenomena such as period-adding bifurcations as a result of “border collision” in the phase space.<sup>10,11</sup> Since our focus is on multistability, we shall consider the weakly dissipative regime and ask what can happen when the Hamiltonian limit is approached. To be concrete, we let  $b$  denote the dissipation parameter, where  $0 \leq |b| \leq 1$  and  $|b|=1$  corresponds to the Hamiltonian limit. What we have found through mathematical analysis and numerical computations is a striking bifurcation route leading to multistability which we call arithmetically period-adding bifurcations. In particular, assume the setting where the system already has a number of coexisting attractors, say for  $b=b_0$ , where  $0 < |b_0| < 1$ . As  $|b|$  is increased from  $|b_0|$ , a sequence of saddle-node bifurcations can occur. At each bifurcation, a periodic attractor appears as a new member of the coexisting attractors. This attractor exists continuously for  $|b| > |b_0|$  and its period is higher than the periods of all attractors that already existed before the bifurcation. The surprising feature is that the sequence constituted by the periods of the new attractors created at the consecutive saddle-node bifurcations is arithmetic. That is, for any given value of  $b$ , the periods of multiple coexisting periodic attractors satisfy an arithmetic rule and, at each saddle-node bifurcation, a periodic attractor is added and its period is arithmetically related to the periods of the existing attractors. The bifurcations thus provide a natural ordering of the coexisting attractors with respect to their periods. To our knowledge, this phenomenon of arithmetically period-adding bifurcations finds no counterpart in smooth dynamical systems, but it is a generic feature associated with multistability in nonsmooth dynamical systems.

In Sec. II, we describe our system model and present numerical evidence for the continuous appearance of arithmetically period-adding attractors. To find the underlying arithmetic rule in period, in Sec. III, we investigate the global dynamics of the system in the Hamiltonian limit. Insight into the dynamical mechanism of arithmetically period-adding bifurcations can be obtained by using symbolic dynamics, which we shall consider in Sec. IV. For specified parameter settings, the existence of coexisting multiple attractors with an arithmetic rule in period can be established rigorously (Sec. V). Conclusions are presented in Sec. VI.

## II. MODEL DESCRIPTION AND NUMERICAL EVIDENCE FOR MULTISTABILITY

We consider a class of two-dimensional piecewise smooth systems with one border and two smooth regions, denoted by  $S_0$  and  $S_1$ , respectively. The systems are introduced as the normal form for border collision bifurcations<sup>10-16</sup> and can be expressed in terms of two affine-subsystems,  $f_0$  and  $f_1$ , as follows:

$$X_{n+1} = F(X_n) = \begin{cases} f_0(X_n), & \text{if } X_n \in S_0, \\ f_1(X_n), & \text{if } X_n \in S_1, \end{cases} \quad (1)$$

where  $X_n = (x_n, y_n) \in \mathbb{R}^2$ ,  $S_0 := \{(x, y) \in \mathbb{R}^2 : x \leq 0, y \in \mathbb{R}\}$  and  $S_1 := \{(x, y) \in \mathbb{R}^2 : x > 0, y \in \mathbb{R}\}$ , and

$$f_0(X_n) = \begin{bmatrix} a & 1 \\ b & 0 \end{bmatrix} \begin{bmatrix} x_n \\ y_n \end{bmatrix} + \begin{bmatrix} \mu \\ 0 \end{bmatrix},$$

$$f_1(X_n) = \begin{bmatrix} c & 1 \\ d & 0 \end{bmatrix} \begin{bmatrix} x_n \\ y_n \end{bmatrix} + \begin{bmatrix} \mu \\ 0 \end{bmatrix}.$$

For notational convenience, we write  $M_0 = \begin{bmatrix} a & 1 \\ b & 0 \end{bmatrix}$  and  $M_1 = \begin{bmatrix} c & 1 \\ d & 0 \end{bmatrix}$ . Here,  $a$  is the trace and  $b$  is the determinant of the Jacobian matrix  $M_0$  of the system at the fixed point in  $S_0$ , and  $c$  is the trace and  $d$  is the determinant of the Jacobian matrix  $M_1$  of the system evaluated at the fixed point in  $S_1$ . To be consistent with our previous works,<sup>14,15</sup> we choose the following parameter setting:

$$a < 0, \quad b < 0, \quad c = -b/a, \quad \text{and} \quad d = b.$$

The area-contracting rate of the map system is  $b$ . The map is dissipative for  $-1 < b < 0$  and conservative for  $b = -1$ . By the natural invariant property of the system dynamics with respect to  $\mu$ ,<sup>13-15</sup> any attractor of the system must contract linearly with  $\mu$ , collapsing to  $(x, y) = (0, 0)$  for  $\mu \rightarrow 0$ . Therefore, the study of dynamics of the map  $F$  for all  $\mu \in \mathbb{R}$  can be reduced to the three cases: (i)  $\mu > 0$ , (ii)  $\mu = 0$ , and (iii)  $\mu < 0$ . As in previous works on multistability in smooth dynamical systems,<sup>6-8</sup> we shall take  $b$  as the bifurcation parameter and investigate the rising of attractors in the regime of weak dissipation as the system approaches the Hamiltonian limit.

To provide numerical evidence for multistability and their appearance through period-adding bifurcations, we fix  $a = -2$  (somewhat arbitrarily) and vary the bifurcation parameter  $b$ . As shown by the bifurcation diagram in Fig. 1, there are multiple coexisting attractors. At each bifurcation point  $b_i$ , a periodic attractor of period  $i$  is born, and the period of the newly born attractor increases as  $b$  is varied toward the Hamiltonian limit  $b = -1$ . For example, the periods of the periodic attractors shown in Fig. 1 are  $3n+2$ , where  $n$  is a non-negative integer. When the system passes through a bifurcation point, the number of multiple coexisting periodic attractors is increased by one. A particular example of multiple coexisting attractors is shown in Fig. 2, for  $b_{11} < b = -0.95 < b_8$ , where three periodic attractors, of period 2, 5, and 8, respectively, together with their basins of attraction, are displayed. We observe that the basins appear to have a quite complicated and interwoven structure, which is typical of multistability even in smooth dynamical systems.<sup>5-8</sup>

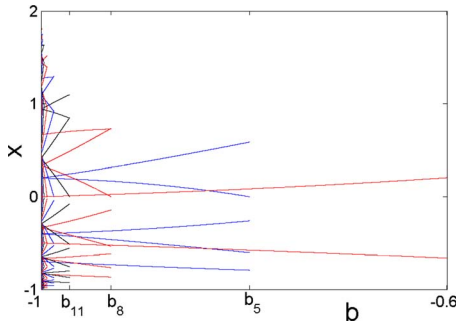


FIG. 1. (Color online) Bifurcation diagram of Eq. (1) for  $a=-2$  showing the occurrence of multiple coexisting periodic attractors. At each bifurcation point  $b_i$ , a new periodic attractor of period  $i$  appears. In fact, the period of any newly appeared attractor is increased arithmetically. The precise values of various  $b_i$  are given in Table I.

Our extensive and systematic numerical computations have revealed the following general features for the nonsmooth system Eq. (1) as the area-contracting rate approaches the Hamiltonian limit from a weakly dissipative regime.

- The dynamics is dominated by a large number of coexisting periodic attractors.
- After a critical bifurcation point  $b_i$ , a periodic attractor as a new member of the family of multiple coexisting attractors appears and exists continuously, that is, once a periodic attractor is created before the Hamiltonian limit, this attractor exists continuously as a stable attractor and it becomes marginally stable at the Hamiltonian limit.
- The period of a newly created periodic attractor after a critical bifurcation point  $b_i$  is higher than the periods of periodic attractors that already existed before the bifurcation point  $b_i$ .
- The sequence of the periods of newly created periodic attractors is arithmetic. For example, in Fig. 1, the sequence is  $\{2, 5, 8, 11, \dots, 3n-1\}$ , where  $n$  is a positive integer. Thus, as the system approaches the Hamiltonian limit, the number of coexisting attractors keeps increasing.
- The higher the period of an attractor, the shorter the interval of the bifurcation parameter  $b$  for its existence. Be-

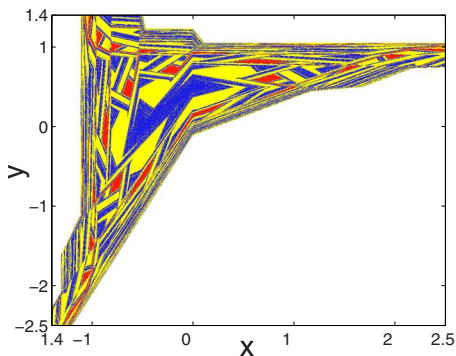


FIG. 2. (Color online) For  $a=-2$  and  $b=-0.95$  in Eq. (1), basins of attraction of three distinct periodic attractors and an additional attractor at infinity. Blank regions indicate the initial conditions that lead to trajectories approaching infinity. The blue, yellow, and red regions denote the basins of the periodic attractors of period 2, 5, and 8, respectively.

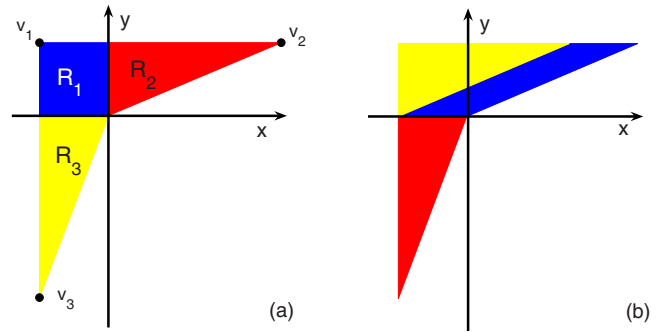


FIG. 3. (Color online) (a) For  $\mu < 0$ , partition of  $B$  into three regions:  $R_1$  (blue),  $R_2$  (red), and  $R_3$  (yellow). Black filled dots indicate the points  $v_1, v_2$ , and  $v_3$ , respectively. (b) First iterations of the respective regions in (a) under the map  $F$ .

cause of this, attractors of higher periods are difficult to detect numerically.

- The basins of attraction of the coexisting attractors are interwoven in a complicated manner, as shown in Fig. 2.

### III. GLOBAL DYNAMICS IN THE HAMILTONIAN LIMIT

Once a periodic attractor appears, it continuously exists as the system approaches the Hamiltonian limit, at which there are marginally stable periodic orbits in various KAM islands whose eigenvalues have magnitude 1. From a different viewpoint, one can imagine moving the system away from the Hamiltonian limit and making it weakly dissipative. The marginally stable orbits then become attractors. To understand the arithmetic rule governing the periods of the attractors, it is insightful to investigate the global dynamics in the corresponding area-preserving, piecewise linear system for  $b=-1$  at which the determinants of two affine-subsystems are one.

#### A. Invariant property

For a given  $\mu \neq 0$ , let  $v_1=(\mu, -\mu)$ ,  $v_2=(a\mu, -\mu)$ ,  $v_3=(\mu, -a\mu)$ , and  $O=(0, 0)$  and let  $B_\mu \subset \mathbb{R}^2$  be the polygon with vertices  $v_1, v_2, O$ , and  $v_3$ . As an example, Fig. 3(a) shows the geometrical shape of  $B_\mu$  for  $\mu < 0$ . In the case in which  $\mu=0$ , we can see that  $B_0=\{0\}$ . Note that the fixed point  $p_\mu$  of the map  $F$  is always in  $B_\mu$ . We can actually show that the set  $B_\mu$  is a maximal invariant set enclosed by heteroclinic saddle connections, as follows.

**Theorem 1.** *If  $b=-1$ , the set  $B_\mu$  is an invariant set of  $F$ , i.e.,  $F(B_\mu)=B_\mu$ .*

*Proof.* To show that  $B_\mu$  is invariant under  $F$ , we partition  $B_\mu$  into three regions  $R_i$ . The first region  $R_1$  is a square with vertices  $(\mu, 0)$ ,  $(\mu, -\mu)$ ,  $(0, -\mu)$  and  $O$ . The second region  $R_2$  (the third region  $R_3$ ) is a triangle with vertices  $O$ ,  $(0, -\mu)$ , and  $(a\mu, -\mu)$  [ $O$ ,  $(\mu, -a\mu)$ , and  $(\mu, 0)$ ], respectively, as shown in Fig. 3(a). The partition of  $B_\mu$  is thus a collection of regions  $R_i$  that are pairwise disjoint except at the boundary points, whose union is  $B_\mu$ , i.e.,

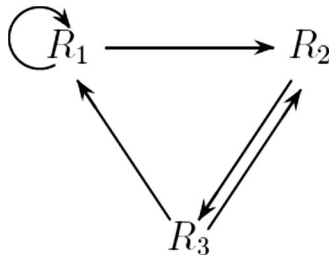


FIG. 4. Transition graph characterizing the dynamics on the invariant set  $B_\mu$  under Eq. (1).

$$B_\mu = R_1 \cup R_2 \cup R_3. \tag{2}$$

Straightforward computations for the image of  $R_i$  under the area-preserving map  $F$  yield the following relations:

$$F(R_1) \subset R_1 \cup R_2, \quad F(R_2) = R_3,$$

$$F(R_3) \subset R_1 \cup R_2, \quad F(R_1 \cup R_3) = R_1 \cup R_2,$$

which imply that  $B_\mu$  is an invariant set of  $F$ . □

When the parameter  $\mu$  is fixed, the invariant set  $B_\mu$  is included in the trapping region of the corresponding dissipative system.<sup>15</sup> For instance, for  $\mu < 0$ , the regions  $R_i$  and its transformations  $F(R_i)$  are illustrated in Fig. 3. To describe the existence of heteroclinic saddle connections, we can examine the existence of a particular saddle periodic orbit.<sup>15</sup>

**Theorem 2.** For  $\mu \neq 0$ ,  $a \neq -1$ , and  $b = -1$ , there exists a periodic saddle orbit  $\{v_1, v_2, v_3\}$ .

*Proof.* For  $\mu \neq 0$ ,  $v_1$  can be iterated under the map  $F$ , which leads to

$$F(v_1) = v_2, \quad F(v_2) = v_3, \quad F(v_3) = v_1. \tag{3}$$

That is,  $\{v_1, v_2, v_3\}$  is a periodic orbit of period 3. To determine the stability of this orbit, we calculate the Jacobian matrix  $DF^3$  of the map  $F^3$ , evaluated at  $v_1$ . We get

$$DF^3(v_1) = \begin{bmatrix} -a & 0 \\ 0 & -1/a \end{bmatrix} \tag{4}$$

for which the eigenvalues are  $\lambda_1 = -a$  and  $\lambda_2 = -1/a$ . The period-3 orbit  $\{v_1, v_2, v_3\}$  is thus a saddle for  $a \neq -1$ . □

Calculation of the stable and the unstable manifolds of each point of the orbit  $\{v_1, v_2, v_3\}$  reveals that they constitute the boundary of  $B_\mu$ ,<sup>17</sup> indicating that the invariant set  $B_\mu$  is only a trapping region, i.e., a trajectory starting outside  $B_\mu$  diverges to infinity. An example of the convex polygon  $B$  for  $\mu < 0$  and its three partitions is shown in Fig. 3(a), and their images under one iteration of the map are shown in Fig. 3(b). Note that, since  $b$  is negative, the map is orientation-preserving. Indeed, as shown in Fig. 3(b), the mappings of the regions  $R_i$  exhibit a counterclockwise pattern of rotation about the origin. The dynamics on  $B_\mu$  can thus be described by the transition graph in Fig. 4, where  $R_i \rightarrow R_j$  means that the intersection of the range of  $R_i$  under the map  $F$  and  $R_j$  is not empty, i.e.,  $F(R_i) \cap R_j \neq \emptyset$ .

The transition graph provides a hint for the occurrence of multiple coexisting periodic attractors having an arithmetic periodicity. In particular, from the graph we immedi-

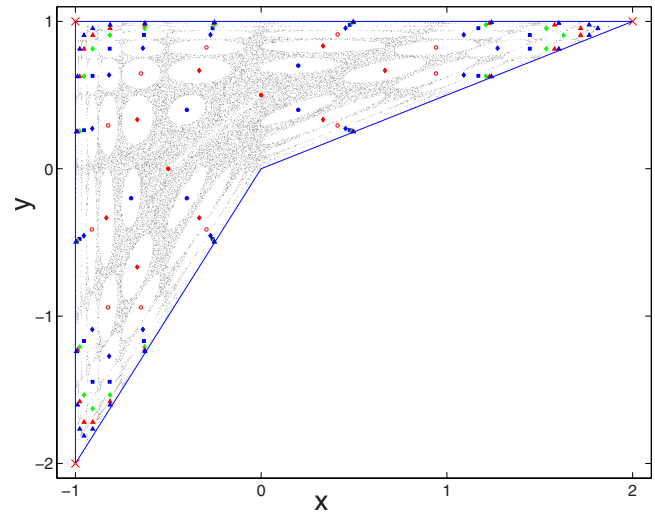


FIG. 5. (Color online) For Eq. (1) in the Hamiltonian limit ( $\mu = -1$ ), chaotic sea, elliptic periodic orbits, and KAM island chains. Blue lines indicate the boundary of the invariant set and markers indicate elliptic periodic orbits in the KAM islands: red crosses for an unstable period-3 orbit, red filled circles for a period-2 orbit, blue filled circles for a period-5 orbit, red filled diamond for a period-8 orbit, red circles for a period-11 orbit, blue filled diamond for a period-14 orbit, blue filled rectangles for a period-17 orbit, green filled diamond for a period-20 orbit, red filled triangles for a period-23 orbit, and blue filled triangles for a period-26 orbit.

ately find a circulating path ( $R_1 \rightarrow R_2 \rightarrow R_3 \rightarrow R_1$ ) of length 3, which is the constant difference in the sequence of periods  $\{2, 5, 8, \dots\}$ .

### B. Chaotic orbits and elliptic islands

There are two distinct types of dynamics on the invariant trapping set  $B_\mu$ : regular and chaotic. The regular dynamics occur in the KAM islands and in the KAM tori embedded in the chaotic sea. The KAM islands are associated with marginally stable periodic orbits whose eigenvalues are equal to 1. A typical phase-space structure of our nonsmooth system in the Hamiltonian limit is shown in Fig. 5, where the KAM islands are represented by blank ellipses in the chaotic sea. A KAM island that contains an elliptic periodic orbit will be converted into a periodic attractor when the system deviates from the Hamiltonian limit and becomes weakly dissipative. As shown in Fig. 5, there are elliptic periodic orbits associated with any particular KAM-island chain. Several observations are as follows: (i) there are unstable periodic orbits associated with every KAM island chain, (ii) a KAM-island chain of lower periodicity is surrounded by a KAM-island chain of higher periodicity, and (iii) KAM-island chains of higher periodicity are located more closely to the boundary of the invariant set. The periods of elliptic periodic orbits in Fig. 5 are  $\{2, 5, 8, 11, 14, 17, 20, 23, 26\}$ , which apparently constitutes an arithmetic sequence. While the detection of some elliptic periodic orbits of higher periods is possible, they stay increasingly close to the boundary and thus are more difficult to visualize. The phase-space structure in Fig. 5 provides a base for the occurrence of a sequence of arithmetically period-adding bifurcations as the system approaches the Hamiltonian limit from the weakly dissipative regime.

**IV. SYMBOLIC DYNAMICS**

The existence of arithmetically period-adding attractors can also be seen by examining the symbolic dynamics of the system defined based on the transition graph in Fig. 4. In particular, the dynamical behavior of the system Eq. (1) is determined by the dynamics of the subsystems,  $f_0$  and  $f_1$ . The existence of a periodic orbit of period  $n$  can be determined by the following set of  $2^n$  equations:

$$X = f_{i_n}(\dots f_{i_2}(f_{i_1}(X)) \dots), \quad i_j \in \{0, 1\}, \quad j = 1, \dots, n. \quad (5)$$

A given orbit  $\{X_m\}$  can be associated with a symbolic sequence  $\{a_m\}$  defined as  $a_m=0$  for  $X_m \in S_0$  and  $a_m=1$  for  $X_m \in S_1$ . Let  $\{p_1, \dots, p_n\}$  be one of the period- $n$  orbits. Its stability is determined by the Jacobian matrix  $DF$  evaluated at the orbit,  $DF = M_{i_1} M_{i_2} \dots M_{i_n}$ , where  $M_{i_j} = DF(p_j)$ .

Our interest is, for any integer  $n \geq 0$ , in the existence of an attracting periodic orbit  $\{p_1, \dots, p_k\}$  of period  $k=3n+2$ . There are three representative closed paths on the transition graph: (i)  $R_3 \rightarrow R_1 \rightarrow R_2 \rightarrow R_3$ , (ii)  $R_3 \rightarrow R_2 \rightarrow R_3$ , and (iii)  $R_1 \rightarrow R_1$ , implying the existence of orbits of periods 3, 2, and 1, respectively. Since the map Eq. (1) is orientation-preserving, there is a general pattern associated with any periodic orbit of period  $k=3n+2$ : it must circulate the first path  $n$  times and then the second path once. For example, a period-8 orbit comes from the following closed path:

$$\begin{array}{ccc} \text{1st path} & \text{1st path} & \text{2nd path} \end{array} \quad (6)$$

$$\overbrace{R_3 \rightarrow R_1 \rightarrow R_2} \rightarrow \overbrace{R_3 \rightarrow R_1 \rightarrow R_2} \rightarrow \overbrace{R_3 \rightarrow R_2} \rightarrow R_3. \quad (7)$$

In the symbolic representation, the three paths can be denoted by (0, 0, 1), (0, 1), and (0), respectively. A periodic orbit of period  $k=3n+2$  can be represented by

$$\underbrace{(0, 0, 1, 0, 0, 1, \dots, 0, 0, 1, 0, 1)}_{3n} \quad (8)$$

$$\underbrace{\phantom{(0, 0, 1, 0, 0, 1, \dots, 0, 0, 1, 0, 1)}}_{+ 2} \quad (9)$$

The corresponding Jacobian matrix  $DF$  is

$$DF = M_0 M_1 (M_0 M_0 M_1)^n.$$

Since

$$M_0 M_1 = \begin{bmatrix} 0 & a \\ -b^2/a & b \end{bmatrix}$$

and

$$M_0 M_0 M_1 = \begin{bmatrix} -(a^2 + b)b/a + ab & a^2 + b \\ 0 & ab \end{bmatrix},$$

an explicit form of the matrix  $DF$  can be obtained through induction,

$$DF = \begin{bmatrix} 0 & a^{n+1} b^n \\ (-1)^{n+1} b^{2(n+1)} a^{-(n+1)} & (-1)^n b^{2n+1} a^{-n} \end{bmatrix}.$$

Its eigenvalues are

$$\lambda_{\pm} = \frac{1}{2} \left( \frac{(-1)^n b^{2n+1}}{a^n} \pm \sqrt{\frac{b^{4n+2}}{a^{2n}} + (-1)^{n+1} 4b^{3n+2}} \right).$$

For  $-1 \leq b < 0$  and  $|a| > 1$ , we have  $|\lambda_{\pm}| < 1$ . The orbit, if it exists, is then stable, corresponding to an attractor.

In the Hamiltonian limit, the eigenvalues become

$$\lambda_i = \frac{1}{2} \left( \frac{(-1)^{n+1}}{a^n} \pm \sqrt{4 - a^{-2n} i} \right),$$

where  $|\lambda_i| = 1$  if  $a < -2^{-n}$ . That is, a periodic attractor becomes an elliptic periodic orbit, as in smooth dynamical systems.

**V. PROOF OF EXISTENCE OF PERIODIC ORBITS**

To be concrete, we fix  $a=-2$  and  $\mu=-1$ , and provide a rigorous analysis for the existence of periodic attractors of arithmetically increasing periods.

**A. Fixed points**

We start by considering the existence and the stability of the fixed point  $p_1$ . A fixed point  $p_1$  is determined by  $X = f_0(X)$  for  $X \in S_0$  and  $X = f_1(X)$  for  $X \in S_1$ , which yields

$$p_1 = \left( \frac{1}{b-3}, \frac{b}{b-3} \right). \quad (10)$$

However, there are no solutions of  $X = f_1(X)$  for  $X \in S_1$ . Since  $p_1 \in S_0$ , the stability of the fixed point is determined by the eigenvalues of the Jacobian matrix  $M_0$  evaluated at  $p_1$ , which are  $-1 \pm \sqrt{1+b}$ . Thus, the fixed point  $p_1$  is a saddle in the relevant parameter range  $b \in (-1, 0)$ .

**B. Period-2 attractors**

To find period-2 orbits for the piecewise linear system Eq. (1), we note that the only possible case is (0, 1), as (1, 0) represents the same case in a binary representation, and (0, 0) and (1, 1) are not possible because there are no period-2 orbits in a linear system. An orbit  $p_2 = (x_2, y_2)$  corresponding to (0, 1) has been found, where

$$x_2 = \frac{b-2}{2(b^2-b+1)} < 0 \quad \text{and} \quad y_2 = \frac{(b^2+b)}{b^2-b+1}.$$

Since  $DF(p_2) = M_1 M_2$ , its eigenvalues are

$$\lambda_i = \frac{b \pm \sqrt{3}|b|i}{2},$$

which are complex number of magnitude  $|\lambda_i| = |b|$ . Thus, for the relevant parameter range  $b \in (-1, 0)$ , the period-2 orbit always exists, and it is an attractor. The period-2 orbit corresponds to the closed path  $R_3 \rightarrow R_2 \rightarrow R_3$  in the symbolic representation.

**C. Period-5 attractors**

By examining the  $2^5$  symbolic sequences that can possibly lead to periodic orbits of period-5, we have found only two such orbits.

**Proposition 1.** *If  $b \leq b_5$ , there exists a stable period-5*

orbit with starting point  $s_5 = (s_{x5}, s_{y5})$  corresponding to a binary sequence  $(0, 0, 1, 0, 1)$  and an unstable orbit  $u_5 = (u_{x5}, u_{y5})$  corresponding to a binary sequence  $(0, 0, 0, 0, 1)$ ,

where the value  $b_5 (\approx -0.794\ 856\ 938\ 437\ 98)$  is a zero of the polynomial  $2b^4 + 4b^3 + 5b^2 + 10b + 6$  in the interval  $[-1, 0]$ ,

$$s_5 = \left( \frac{2b^4 + 4b^3 + 3b^2 + b + 2}{2b^5 + b^3 - 2}, \frac{2b^5 + 5b^4 + 8b^3 + 4b^2 - 2b}{2b^5 + b^3 - 2} \right) \tag{11}$$

for  $s_{x5} < 0$  and  $s_{y5} < 0$ , and

$$u_5 = \left( \frac{2b^4 + 6b^3 + 15b^2 + 17b + 2}{2b^5 + b^3 - 4b^2 - 16b - 2}, \frac{2b^5 + 6b^4 + 18b^3 + 34b^2 + 22b}{2b^5 + b^3 - 4b^2 - 16b - 2} \right) \tag{12}$$

for  $u_{x5} < 0$  and  $u_{y5} < 0$ .

**Proof.** Starting from the point  $s_5$  under the binary sequence  $(0, 0, 1, 0, 1)$ , we get the following iterated points:

$$\begin{aligned} s_5^1 &\equiv f_0(s_5) = \left( \frac{b^4 - b^3 - 2b^2 - 4b - 2}{2b^5 + b^3 - 2}, \frac{2b^5 + 4b^4 + 3b^3 + b^2 + 2b}{2b^5 + b^3 - 2} \right), \\ s_5^2 &\equiv f_0(s_5^1) = \left( \frac{2b^4 + 4b^3 + 5b^2 + 10b + 6}{2b^5 + b^3 - 2}, \frac{b^5 - b^4 - 2b^3 - 4b^2 - 2b}{2b^5 + b^3 - 2} \right), \\ s_5^3 &\equiv f_1(s_5^2) = \left( \frac{2b^4 - b^3 + 2b^2 + 2b + 4}{2(2b^5 + b^3 - 2)}, \frac{2b^5 + 4b^4 + 5b^3 + 10b^2 + 6b}{2b^5 + b^3 - 2} \right), \\ s_5^4 &\equiv f_0(s_5^3) = \left( \frac{2b^4 + 5b^3 + 8b^2 + 4b - 2}{2b^5 + b^3 - 2}, \frac{2b^5 - b^4 + 2b^3 + 2b^2 + 4b}{2(2b^5 + b^3 - 2)} \right), \\ s_5 &= f_1(s_5^4) = \left( \frac{2b^4 + 4b^3 + 3b^2 + b + 2}{2b^5 + b^3 - 2}, \frac{2b^5 + 5b^4 + 8b^3 + 4b^2 - 2b}{2b^5 + b^3 - 2} \right). \end{aligned}$$

As stipulated by the dynamics, the points will constitute a period-5 orbit if they are in their respectively proper regions,

$$s_5 \in S_0, \quad s_5^1 \in S_0, \quad s_5^2 \in S_1, \quad s_5^3 \in S_0, \quad \text{and} \quad s_5^4 \in S_1.$$

Since the polynomial  $2b^5 + b^3 - 2$  is negative on the interval  $[-1, 0]$ , for the existence of such a periodic orbit, we obtain the following conditions:

$$\begin{aligned} b^4 - b^3 - 2b^2 - 4b - 2 > 0, \quad 2b^4 + 4b^3 + 5b^2 + 10b + 6 < 0, \quad 2b^4 - b^3 + 2b^2 + 2b + 4 > 0, \\ 2b^4 + 5b^3 + 8b^2 + 4b - 2 < 0, \quad 2b^4 + 4b^3 + 3b^2 + b + 2 > 0, \end{aligned}$$

which are all satisfied on the interval  $[-1, b_5]$ , where  $b_5$  is a zero of  $2b^4 + 4b^3 + 5b^2 + 10b + 6$  on the interval  $[-1, 0]$  ( $b_5 \approx -0.794\ 856\ 938\ 437\ 98$ ). Thus, for  $b \leq b_5$ , the orbit that starts from  $s_5$  is a periodic orbit of period 5. The corresponding Jacobian matrix  $DF(s_5)$  is

$$DF = M_1 M_0 M_1 M_0 M_0 = \begin{bmatrix} 2b^2 + b^3/2 & -b^2 \\ 4b^2 & -2b^2 \end{bmatrix}$$

and the eigenvalues are

$$\lambda_i = \frac{1}{2} \left( \frac{b^3}{2} \pm \sqrt{\frac{b^6}{4} + 4b^5} \right).$$

The magnitudes of eigenvalues  $\lambda_i$  are  $|b^5|$ . We thus obtain  $|\lambda_i| < 1$  for  $b \in (-1, b_5]$  and, hence, the orbit is stable.

Similarly, by iterating the point  $u_5$ , we obtain

$$\begin{aligned} u_5^1 &\equiv f_0(u_5) = \left( \frac{2b^4 + 5b^3 + 8b^2 + 4b - 2}{2b^5 + b^3 - 4b^2 - 16b - 2}, \frac{2b^5 + 6b^4 + 15b^3 + 17b^2 + 2b}{2b^5 + b^3 - 4b^2 - 16b - 2} \right), \\ u_5^2 &\equiv f_0(u_5^1) = \left( \frac{2b^4 + 4b^3 + 5b^2 + 10b + 6}{2b^5 + b^3 - 4b^2 - 16b - 2}, \frac{2b^5 + 5b^4 + 8b^3 + 4b^2 - 2b}{2b^5 + b^3 - 4b^2 - 16b - 2} \right), \end{aligned}$$

$$u_5^3 \equiv f_0(u_5^2) = \left( \frac{b^4 - b^3 - 2b^2 - 6b - 10}{2b^5 + b^3 - 4b^2 - 16b - 2}, \frac{2b^5 + 4b^4 + 5b^3 + 10b^2 + 6b}{2b^5 + b^3 - 4b^2 - 16b - 2} \right),$$

$$u_5^4 \equiv f_0(u_5^3) = \left( \frac{2b^4 + 6b^3 + 18b^2 + 34b + 22}{2b^5 + b^3 - 4b^2 - 16b - 2}, \frac{b^5 - b^4 - 2b^3 - 6b^2 - 10b}{2b^5 + b^3 - 4b^2 - 16b - 2} \right),$$

$$u_5 = f_1(u_5^4) = \left( \frac{2b^4 + 6b^3 + 15b^2 + 17b + 2}{2b^5 + b^3 - 4b^2 - 16b - 2}, \frac{2b^5 + 6b^4 + 18b^3 + 34b^2 + 22b}{2b^5 + b^3 - 4b^2 - 16b - 2} \right).$$

The orbit  $(u_5, u_5^1, u_5^2, u_5^3, u_5^4)$  will be a periodic orbit if the following conditions are satisfied:

$$u_5 \in S_0, \quad u_5^1 \in S_0, \quad u_5^2 \in S_0, \quad u_5^3 \in S_0, \quad \text{and} \quad u_5^4 \in S_1. \tag{13}$$

Since  $2b^4 + 5b^3 + 8b^2 + 4b - 2 < 0$  for  $b \in [-1, 0]$ , the value  $2b^5 + b^3 - 4b^2 - 16b - 2$  should be positive in order to satisfy  $u_5^1 \in S_0$ . We obtain that  $2b^5 + b^3 - 4b^2 - 16b - 2 > 0$  for  $b \in [-1, c]$ , where  $c \approx -0.129\ 320\ 649\ 810\ 92$ . The conditions in Eq. (13) thus become

$$2b^4 + 4b^3 + 5b^2 + 10b + 6 < 0,$$

$$b^4 - b^3 - 2b^2 - 6b - 10 < 0,$$

$$2b^4 + 6b^3 + 18b^2 + 34b + 22 > 0,$$

$$2b^4 + 6b^3 + 15b^2 + 17b + 2 < 0.$$

It can be checked that all the inequalities are satisfied for  $b \in [-1, b_5]$ . There is then a second period-5 orbit for  $b \in [-1, b_5]$ . The product of the Jacobian matrices evaluated at the orbital points is

$$DF(u_5) = M_1 M_0 M_0 M_0 M_0$$

$$= \begin{bmatrix} b^2(4+b)/2 & -b^2 \\ b^3 + 12b^2 + 16b & -8b - 4b^2 \end{bmatrix},$$

which gives the eigenvalues

$$\lambda_{\pm} = -\frac{4b^2 - b^3 + 16b \pm b\sqrt{b^4 + 8b^3 - 16b^2 + 128b + 256}}{4}$$

with  $3 < \lambda_+ < 6$  and  $0 < \lambda_- < 1$  on interval  $[-1, b_5]$ . This period-5 orbit is thus unstable (a saddle). □

We remark that at the critical bifurcation point  $b_5$ , the iterating points  $s_5^2$  and  $u_5^2$  are the same and are on the border. Proposition 1 thus indicates that a point on the border line breaks up; two points drift apart. As a result, two periodic orbits of period-5 appear as  $b$  is decreased through  $b_5$ , one stable and another unstable. There is a saddle-node bifurcation at  $b_5$ .

#### D. Periodic attractor of period 8

By examining the  $2^8$  symbolic sequences that can possibly lead to periodic orbits of period-8, we have found four such orbits. Their corresponding symbolic codes are  $(0, 0, 1, 0, 0, 1, 0, 1)$  for a stable orbit, and  $(0, 0, 0, 0, 0, 0, 0, 1)$ ,  $(0, 0, 1, 0, 0, 0, 0, 1)$ , and  $(0, 0, 0, 0, 0, 1, 0, 1)$  for unstable orbits.

**Proposition 2.** For  $b \leq b_8$ , there exist a stable period-8 orbit with starting point  $s_8 = (s_{x8}, s_{y8})$  corresponding to the binary sequence  $(1, 0, 1, 0, 0, 1, 0, 0)$  and an unstable period-8 orbit  $u_8 = (u_{x8}, u_{y8})$  corresponding to the binary sequence  $(0, 0, 1, 0, 0, 1, 0, 0)$ , where the value  $b_8 (\approx -0.931\ 205\ 981\ 564\ 08)$  is a zero of the polynomial  $4b^7 + 8b^6 + 8b^5 + 15b^4 + 14b^3 + 30b^2 + 12b - 12$  in the interval  $[-1, 0]$ ,

$$s_{x8} = \frac{4b^7 + 8b^6 + 8b^5 + 15b^4 + 14b^3 + 30b^2 + 12b - 12}{4b^8 - b^5 + 4}, \tag{14}$$

$$s_{y8} = \frac{b(2b^7 - 2b^6 - 5b^5 - 8b^4 - 8b^3 - 16b^2 - 8b + 4)}{4b^8 - b^5 + 4}, \tag{15}$$

$$u_{x8} = \frac{4b^7 + 8b^6 + 8b^5 + 15b^4 + 14b^3 + 30b^2 + 12b - 12}{4b^8 - b^5 - 16b^3 - 64b^2 + 4}, \tag{16}$$

and

$$u_{y8} = \frac{b(b^8 + 3b^7 + 9b^6 + 27b^5 + 79b^4 + 173b^3 + 199b^2 + 85b)}{4b^7 + 10b^6 + 15b^5 + 16b^4 + 32b^3 + 16b^2 + 4}. \tag{17}$$

At the critical bifurcation point  $b_8$ , two starting points  $s_8$  and  $u_8$  are the same.

**Proof.** Similar to the proof of Proposition 1.

Note that  $(1, 0, 1, 0, 0, 1, 0, 0) = (0, 0, 1, 0, 0, 1, 0, 1)$  and  $(0, 0, 1, 0, 0, 1, 0, 0) = (0, 0, 1, 0, 0, 0, 0, 1)$  in the symbolic representation. Proposition 2 shows that there is a saddle-node bifurcation at  $b_8$ .

#### E. Periodic attractor of period 11

By examining the  $2^{11}$  symbolic sequences that can possibly lead to periodic orbits of period-11, we have found four such orbits. Their symbolic codes are  $(0, 0, 1, 0, 0, 1, 0, 0, 1, 0, 1)$  for stable orbits, and  $(0, 0, 0, 0, 0, 0, 0, 0, 0, 0, 1)$ ,  $(0, 0, 1, 0, 0, 1, 0, 0, 0, 0, 1)$ , and  $(0, 0, 0, 0, 0, 0, 0, 0, 1, 0, 1)$  for unstable orbits.

**Proposition 3.** For  $b \leq b_{11}$ , there exist a stable period-8 orbit with starting point  $s_{11}=(s_{x11},s_{y11})$  corresponding to the binary code (1, 0, 1, 0, 0, 1, 0, 0, 1, 0, 0) and an unstable period-8 orbit  $u_{11}=(u_{x11},u_{y11})$  corresponding to the binary

code (0, 0, 1, 0, 0, 1, 0, 0, 1, 0, 0), where the value  $b_{11}(\approx -0.971\ 920\ 725\ 938\ 61)$  is a zero of the polynomial  $8b^{10}+16b^9+16b^8+32b^7+33b^6+66b^5+66b^4+132b^3+68b^2-24b+24$  in the interval  $[-1,0]$ ,

$$s_{x11} = \frac{8b^{10} + 16b^9 + 16b^8 + 32b^7 + 33b^6 + 66b^5 + 66b^4 + 132b^3 + 68b^2 - 24b + 24}{8b^{11} + b^7 - 8}, \tag{18}$$

$$s_{y11} = \frac{b(4b^{10} - 4b^9 - 10b^8 - 15b^7 - 16b^6 - 32b^5 - 32b^4 - 64b^3 - 32b^2 + 16b - 8)}{8b^{11} + b^7 - 8}, \tag{19}$$

$$u_{x11} = \frac{8b^{10} + 16b^9 + 16b^8 + 32b^7 + 33b^6 + 66b^5 + 66b^4 + 132b^3 + 68b^2 - 24b + 24}{8b^{11} + b^7 - 64b^4 - 256b^3 - 8}, \tag{20}$$

and

$$u_{y11} = \frac{b(8b^{10} + 20b^9 + 30b^8 + 33b^7 + 64b^6 + 64b^5 + 128b^4 + 64b^3 - 32b^2 + 16b - 8)}{8b^{11} + b^7 - 64b^4 - 256b^3 - 8}. \tag{21}$$

At the critical bifurcation point  $b_{11}$ , two starting points  $s_{11}$  and  $u_{11}$  are the same.

**Proof.** Similar to the proof of Proposition 1. Note that

$$(1,0,1,0,0,1,0,0,1,0,0) = (0,0,1,0,0,1,0,0,1,0,1)$$

and

$$(0,0,1,0,0,1,0,0,1,0,0) = (0,0,1,0,0,1,0,0,0,0,1)$$

in the symbolic representation. Proposition 3 shows that there is a saddle-node bifurcation at  $b_{11}$ .

TABLE I. Existence and stability of periodic orbits, and critical bifurcating point of attracting periodic orbits.

Period	Existence	Stability	Bifurcation point
1	Exist	Unstable	
2	Exist	Stable	$b_2 < 0$
3	Exist	Unstable	
4	Not Exist		
5	Exist	Stable/Unstable	$b_5 \approx -0.794\ 8$
6	Not Exist		
7	Exist	Unstable	
8	Exist	Stable/Unstable	$b_8 \approx -0.931\ 2$
9	Exist	Unstable	
10	Exist	Unstable	
11	Exist	Stable/Unstable	$b_{11} \approx -0.971\ 9$
12	Exist	Unstable	
13	Exist	Unstable	
14	Exist	Stable/Unstable	$b_{14} \approx -0.987\ 5$
15	Exist	Unstable	
16	Exist	Unstable	
17	Exist	Stable/Unstable	$b_{17} \approx -0.994\ 2$
18	Exist	Unstable	
19	Exist	Unstable	
20	Exist	Stable/Unstable	$b_{20} \approx -0.997\ 2$
21	Exist	Unstable	
22	Exist	Unstable	
23	Exist	Stable/Unstable	$b_{23} \approx -0.998\ 65$
24	Exist	Unstable	
25	Exist	Unstable	
26	Exist	Stable/Unstable	$b_{26} \approx -0.999\ 3$

**F. Periodic orbits of higher periods**

We have so far considered the existence and stabilities of periodic orbits of periods 1, 2, 5, 8, and 11. Propositions 1, 2, and 3 indicate that these periodic orbits are created by saddle-node bifurcations. The symbolic codes for the stable and the unstable orbits are

$$\underbrace{(0,0,1,0,0,1, \dots, 0,0,1)}_{3n} + \underbrace{(0,1)}_2,$$

$$\underbrace{(0,0,1, \dots, 0,0,1)}_{3(n-1)} + \underbrace{(0,0,0)}_3 + \underbrace{(0,1)}_2,$$

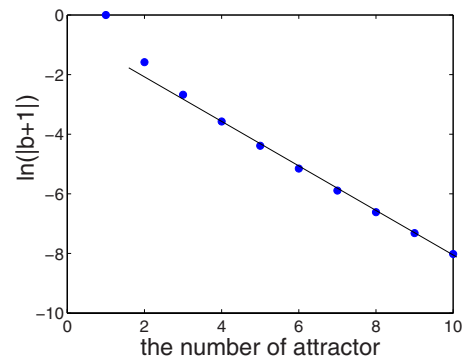


FIG. 6. (Color online) The number of attractors vs  $\ln(|b+1|)$  as the Hamiltonian limit is approached.

respectively. We have analyzed the existence and the stabilities of periodic orbits of period up to 26. The results are summarized in Table I.

### G. Scaling of the number of attractors

As the Hamiltonian limit is approached (i.e.,  $|b+1| \rightarrow 0$ ), the number of attractors increases. Numerically we find that this number scales with  $|b+1|$  as  $\ln(|b+1|)$ , as shown in Fig. 6. It appears difficult at the present to obtain this scaling law theoretically.

## VI. CONCLUSIONS

We have addressed the problem of multistability in piecewise smooth dynamical systems. The two facts that motivate our work are (i) multistability has been an interesting topic in nonlinear dynamics<sup>4-8</sup> and (ii) nonsmooth dynamical systems arise commonly in physical and engineering applications and they permit behaviors that usually find no counterparts in smooth systems.<sup>10-16</sup> By considering a generic class of piecewise smooth dynamical systems that have been the paradigm for studying nonsmooth dynamics and by focusing on the weakly dissipative regime and the Hamiltonian limit, we find that multistability, in the form of multiple coexisting periodic attractors, is quite common and we identify the saddle-node bifurcation as the mechanism to create various periodic attractors. While saddle-node bifurcations are common in smooth dynamical systems, a striking phenomenon for piecewise smooth systems is that, as the Hamiltonian limit is approached, the periods of the newly created periodic attractors follow an arithmetic sequence. We have provided physical analyses, numerical computations, and mathematical proofs to establish our finding. To our knowledge, the phenomenon of arithmetically period-adding bifurcations has no counterpart in smooth dynamical systems.

Nonsmooth dynamical systems are of particular interest in physical and engineering applications.<sup>2,3</sup> From the standpoint of dynamics, they often permit interesting and surprising phenomena. Our work is a further illustration of this fact

with respect to the problem of multistability. We hope our finding will stimulate further research in this interesting area of nonlinear dynamics.

## ACKNOWLEDGMENTS

Y.-C.L. is supported by AFOSR under Grant No. FA9550-06-1-0024. Y.D. is supported by a Korea Research Foundation Grant funded by the Korean Government (MOE-HRD, Basic Research Promotion Fund) (Grant No. KRF-2008-331-C00023).

<sup>1</sup>Special issue on Multistability in Dynamical Systems, Int. J. Bifurcation Chaos Appl. Sci. Eng. **18** (2008).

<sup>2</sup>See, for example, J. M. T. Thompson and R. Ghaffari, *Phys. Rev. A* **27**, 1741 (1983); S. W. Shaw and P. J. Holmes, *J. Sound Vib.* **90**, 129 (1983); G. S. Whiston, *ibid.* **118**, 395 (1987); A. B. Nordmark, *ibid.* **145**, 279 (1983); W. Chin, E. Ott, H. E. Nusse, and C. Grebogi, *Phys. Rev. E* **50**, 4427 (1994); F. Casas, W. Chin, C. Grebogi, and E. Ott, *ibid.* **53**, 134 (1996).

<sup>3</sup>See, for example, S. Banerjee, J. A. Yorke, and C. Grebogi, *Phys. Rev. Lett.* **80**, 3049 (1998); S. Banerjee and C. Grebogi, *Phys. Rev. E* **59**, 4052 (1999); S. Banerjee, P. Ranjan, and C. Grebogi, *IEEE Trans. Circuits Syst., I: Fundam. Theory Appl.* **47**, 633 (2000); S. Parui and S. Banerjee, *ibid.* **50**, 1464 (2003); S. Banerjee, S. Parui, and A. Gupta, *IEEE Trans. Circuits Syst., II: Express Briefs* **51**, 649 (2004).

<sup>4</sup>P. M. Battelino, C. Grebogi, E. Ott, and J. A. Yorke, *Physica D* **32**, 296 (1988).

<sup>5</sup>U. Feudel, C. Grebogi, B. Hunt, and J. A. Yorke, *Phys. Rev. E* **54**, 71 (1996).

<sup>6</sup>U. Feudel and C. Grebogi, *Chaos* **7**, 597 (1997).

<sup>7</sup>S. Kraut, U. Feudel, and C. Grebogi, *Phys. Rev. E* **59**, 5253 (1999).

<sup>8</sup>U. Feudel and C. Grebogi, *Phys. Rev. Lett.* **91**, 134102 (2003).

<sup>9</sup>M. Dutta, H. E. Nusse, E. Ott, J. A. Yorke, and G.-H. Yuan, *Phys. Rev. Lett.* **83**, 4281 (1999); A. Ganguli and S. Banerjee, *Phys. Rev. E* **71**, 057202 (2005).

<sup>10</sup>H. E. Nusse and J. A. Yorke, *Physica D* **57**, 39 (1992).

<sup>11</sup>H. E. Nusse, E. Ott, and J. A. Yorke, *Phys. Rev. E* **49**, 1073 (1994).

<sup>12</sup>S. Parui and S. Banerjee, *Chaos* **12**, 1054 (2002).

<sup>13</sup>M. A. Hassouneh, E. H. Abed, and H. E. Nusse, *Phys. Rev. Lett.* **92**, 070201 (2004).

<sup>14</sup>Y. Do and H. H. Baek, *Commun. Pure Appl. Anal.* **5**, 493 (2006).

<sup>15</sup>Y. Do, *Chaos, Solitons Fractals* **32**, 352 (2007).

<sup>16</sup>V. Avrutin, M. Schanz, and S. Banerjee, *Phys. Rev. E* **75**, 066205 (2007).

<sup>17</sup>H. K. Baek and Y. Do, "Existence of homoclinic orbits on an area-preserving map with a nonhyperbolic invariant set," *Chaos, Solitons Fractals* (in press).